ADVANCED OPTICAL MATERIALS
www.advopticalmat.de

Structural Color Manipulation Using Tunable Photonic Crystals with Enhanced Switching Reliability

Moon Gyu Han, Chul-Joon Heo, Hongshik Shim, Chang Gyun Shin, Seon-Jeong Lim, Jung Woo Kim, Yong Wan Jin, and Sangyoon Lee**

Photonic crystals are periodically structured materials in which refractive indices are spatially modulated, creating a stop-band into the optical band structure so that photons at certain energies cannot propagate.[1] This ability to control light propagation makes them useful in many applications.[2] Furthermore, the position of a stop-band can be modulated by tuning the refractive index and/or the periodicity of the photonic-crystal structure. Such photonic crystals are called tunable photonic crystals. In particular, tunable photonic crystals that show stop-bands in the visible or near-infrared region are of special interest for their ability to control light for use in active components of displays, sensors, or other optical devices.[3–5]

Although developing various types of tunable photonic crystals, many of which are based on colloidal crystals, has recently been a subject of much interest in the materials science community,[6] fabricating reproducible and robust tunable photonic crystals remains challenging because the poor repeatability of the stop-band tuning limits their practical application. There have been several reports to date on tunable photonic crystals that show repeatable stop-band tuning. Ozin et al. reported 100 times of stable switching with stop-band tuning range ($\Delta\lambda$) of around 100 nm through oxidation/reduction reaction using EAP-infiltrated photonic crystal.[3a] Kang et al. reported 30 times of switching with tuning range of about 75 nm using block-copolymer photonic gel for application to non-volatile display pixels.[7] Li et al. developed a polymeric ionic liquid (PIL)-based integrated photonic crystal that showed 10 stable tuning cycles.[8]

In contrast to closely packed photonic structures, crystalline colloidal arrays, which are periodically arranged non-close-packed colloidal arrays dispersed in solvent media, i.e. water, through electrostatic repulsive forces between charged particles,[9] allow for changes in their lattice spacing simply by manipulating the volume fractions of the particles in a dispersion medium. This phenomenon has recently been judiciously exploited to tune lattice constants by manipulating external fields, which has led to a wide range of photonic stop-band tuning in the whole visible regime through large changes in the particle-particle separation originating from the electrophoretic movement of the charged particles while maintaining the ordered crystal structure under the external fields.[10] In spite of these merits, there is no report that considered these systems applicable for reversible switching for practical application.

Although de-ionized water is the most suitable dispersion medium for producing high quality periodic crystalline structures with enhanced reflectance in these systems, the electrolysis of water molecules at the indium tin oxide (ITO) surface produces significant amounts of H^+ and OH^- ions as by-products at the cathode and anode, respectively. Therefore, the diffusion of those ions into colloidal arrays substantially limits the tuning stability and range because this phenomena induces decreased thickness of electrical double layer on the surface of the colloidal nanoparticles. To solve this problem, ITO surface was modified by various dielectric insulator passivation layers, including SiO_2, SiN, polyimide, and parylene that can block electrochemical reactions at the electrodes (unpublished results). However, this methodology resulted in a substantial reduction of the color tuning range due to decreases in voltage applied to the colloidal dispersion because of the large amount of additional impedance introduced by the passivation layer. Considering the volume resistivity of these commonly used passivation materials (~10^{16} Ω m), required thickness of the passivation layer should be at the sub-nm scale in order not to decrease the voltage applied significantly in colloidal dispersion. Preparation of such a thin and uniform film without any defected area is extremely difficult to achieve.

Here we report our effort for achieving enhanced tuning stability of the colloidal photonic crystal composed of long-range ordered crystalline colloidal arrays through modifying the ITO electrode with ion exchange resins. The thin layer of over-coating on the ITO surface allowed increased number of cycles of stable color-tuning switching from red to green over 800 times, which is the best result ever reported for a tunable photonic crystal whose $\Delta\lambda$ can be manipulated more than 100 nm.

Figure 1(a) depicts the device structure of a unit pixel and the concept of improving the stability of photonic structural color tuning through blocking ion diffusion from both electrodes by coating the electrode surface with a layer of ion-exchange resin. A colloidal dispersion composed of monodisperse 138 nm-diameter polystyrene (PS) nanoparticles dispersed in deionized water was injected between two electrodes. The strong negative charge of the nanoparticles and their thick electrical double layer induce the self-assembly of the long-range ordered colloids through electrostatic repulsion, which dominates the

Dr. M. G. Han, Dr. C.-J. Heo, H. Shim, Dr. C. G. Shin, Dr. S.-J. Lim, Dr. J. W. Kim, Dr. Y. W. Jin, Dr. S. Lee
Organic Materials Lab.,
Samsung Advanced Institute of Technology
Samsung Electronics,
130 Samsung-ro, Suwon,
Gyeonggi-do 443-803, South Korea
E-mail: moongyu.han@samsung.com; sangyoon.lee@samsung.com

DOI: 10.1002/adom.201400038

© 2014 WILEY-VCH Verlag GmbH & Co. KGaA, Weinheim

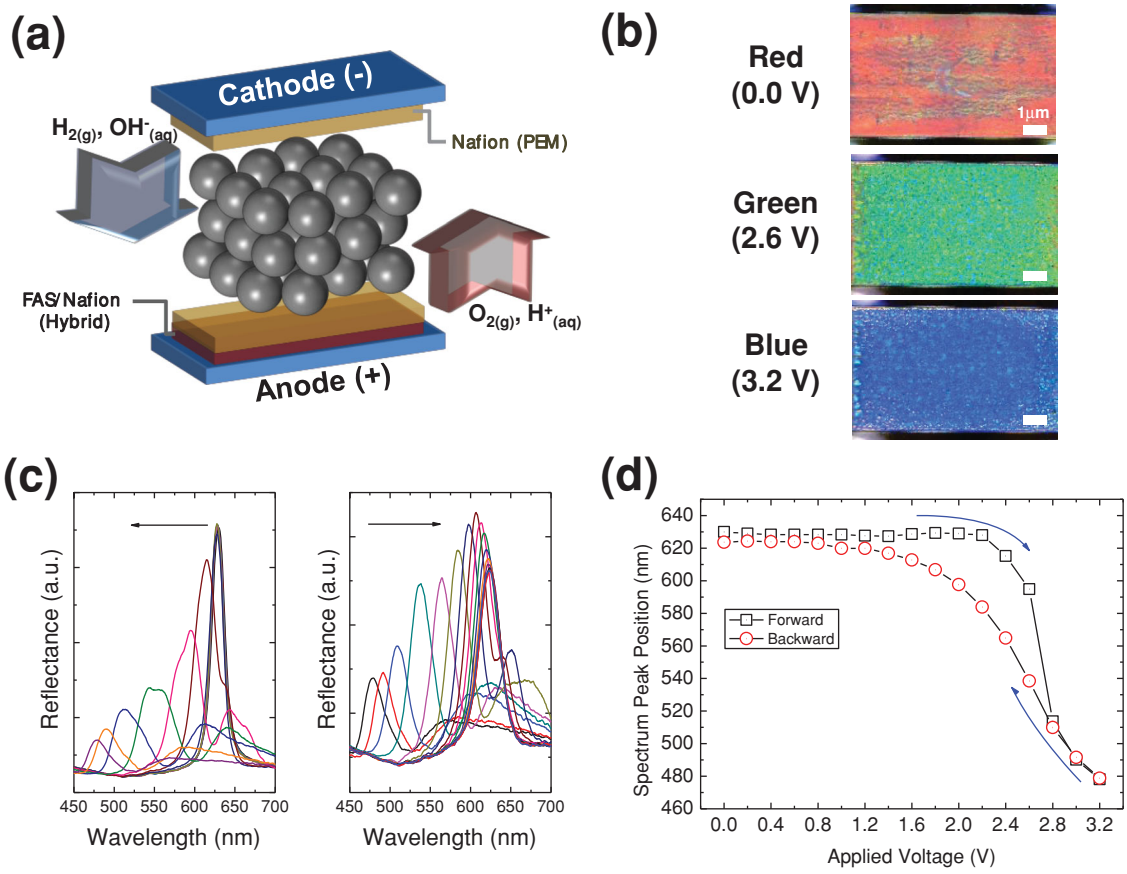

Figure 1. (a) Schematic depiction of a crystalline colloid assembly (CCA) under an electric field in an electrode assembly. The surfaces of both electrodes were modified with ion-exchange membranes to increase the electrochemical stability of the electrodes during color modulation. (b) Optical images of the CCA in the electrode assembly were tuned by varying the electrical field. Red, green, and blue were expressed from the CCA by applying 0, 2.6, and 3.2 V, respectively. (c) Reflectance spectra obtained during voltage sweep: From 0 to 3.2 V (left) and from 3.2 to 0 V (right). The voltage was swept at 0.1 V/s to generate both spectra. (d) Peak position plotted as functions of applied voltage: Black squares and red circles represent results obtained during forward and backward operations, respectively.

nanoparticle interactions described by Derjaguin-Landau-Verwey-Overbeek (DLVO) theory. The particle concentration and the resulting inter-particle distance determine the periodicity of the assembled structures and the structural color. The photonic color could be precisely tuned from red to blue by increasing the applied potential from 0 to 3.2 V, as is shown in Figure 1(b). The mechanism for the photonic color tuning is based on the electrophoretic movement of the colloidal nanoparticles to the anode and locally increased particle concentration while maintaining the ordered crystal structure through the electrostatic repulsion between adjacent particles, when potential is applied between the two electrodes. Balancing the dominant electrophoretic and electrostatic repulsion forces for certain applied voltages leads to various colors being expressed at those potentials. The reflection peak due to the photonic stop-band systematically moves from a longer wavelength to a shorter one with increasing applied voltage, as is shown in Figure 1(c). In this experiment, the voltage was swept at 0.1 V/s, which was optimized to exhibit the maximum tuning range (see Supporting Information Figure S1). During backward operation, in which the applied voltage diminishes, the decreased electrophoretic force of the nanoparticles lead to the increase of the inter-particle distance. Therefore, the stop-band position systematically recovers from blue to red, leading to a finely tuned, reversible manipulation of the stop-band by varying the applied voltage, as is shown in Figure 1(d). There exists a threshold voltage (2.2 V) during forward operation, below which the stop-band position seldom moves to a shorter wavelength. This threshold is supposed to be due to the strong resistance against the particles moving closer to each other owing to the dominant electrostatic repulsion between particles at voltages below 2.2 V. The stop-band position dramatically moves to a shorter wavelength with increasing voltage above 2.2 V. In this condition, electrophoretic force contributed significantly to the tuning behavior. During backward operation, however, there is no threshold-like behavior because backward operation is a relaxation procedure. This difference leads to some hysteresis between the forward and backward operations, as is clearly shown in Figure 1(d).

The energy barrier that must be surmounted to charge separation in water is much less than the one in organic solvents because of the high dielectric constant (≈80) of water molecules and thus short Bjerrum length (~0.7 nm). Therefore, the strong surface charge (zeta potential = −72.05 mV) of the particle in deionized water readily allows to form stable crystalline colloidal

© 2014 WILEY-VCH Verlag GmbH & Co. KGaA, Weinheim

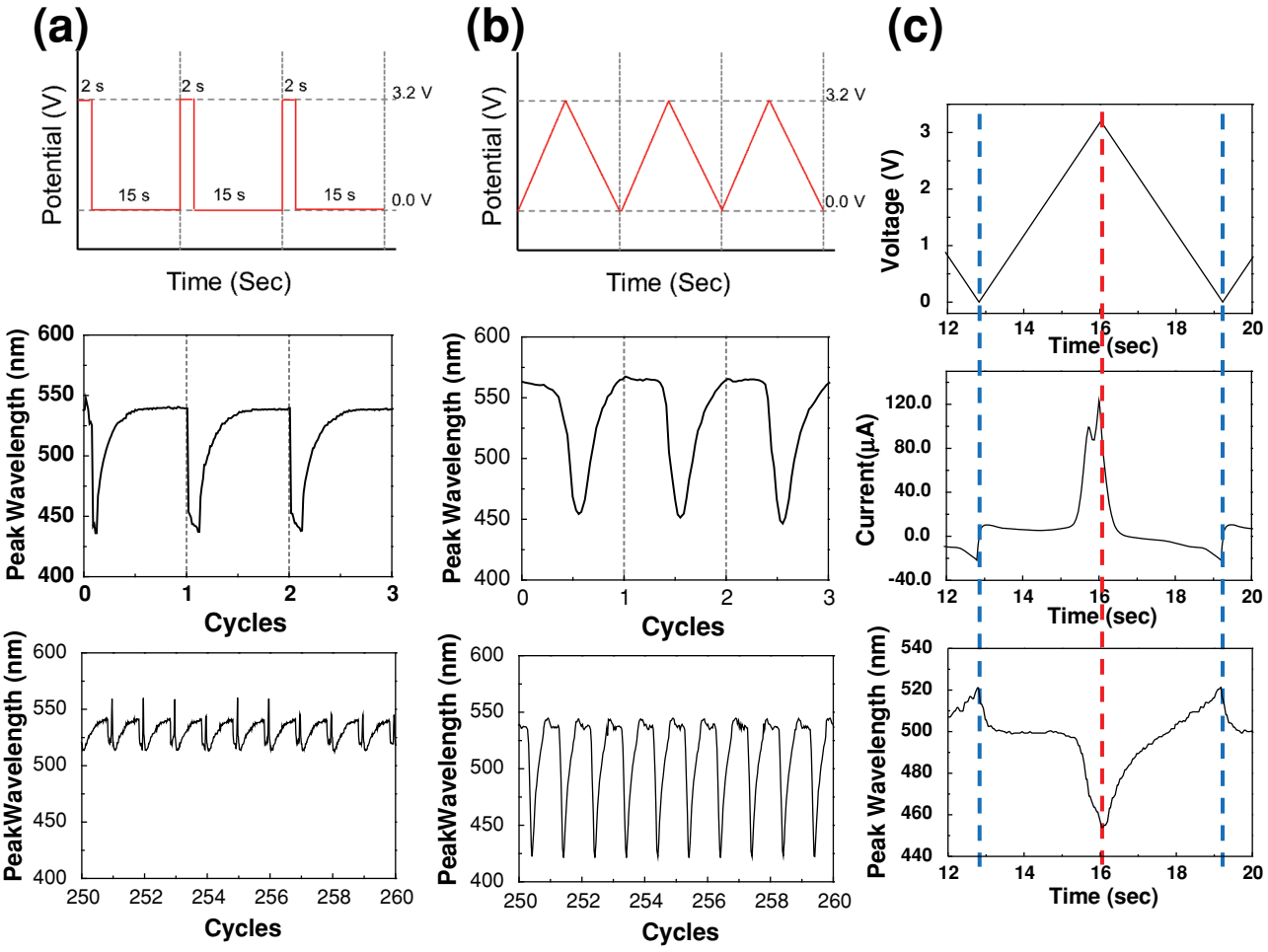

Figure 2. Dynamic properties of CCA measured under certain operation conditions: (a) pulse-like operation, (b) sweeping voltage (sweeping rate: 1 V/s). The reflectance peak wavelength was recorded and analyzed as functions of time and voltage under both operation conditions. The top figures in (a,b) show the applied potential plotted as functions of time, the middle graphs represent wavelength tuning during the first 3 cycles, and the bottom graphs show the results of the wavelength tuning after 250 switching cycles. (c) Real-time analysis of the nanoparticle-movement-induced current flow and the corresponding changes in the positions of the spectrum peaks with applied voltage. The ITO electrodes were modified with the same configuration described in Figure 1(a). The switching area of the unit cell device was 100 mm^2.

arrays having electrically tunable, strong reflective color characteristics. However, one problem of colloidal nanoparticles dispersed in water is the poor tuning repeatability originated from unwanted ion generation at the electrode surface and its diffusion into the colloidal dispersion when the applied potential is above the minimum potential required for reduction and oxidation, as is simulated by COMSOL multiphysics (see Figure S2). Owing to the decreased surface charge and electrophoretic movement caused by the production of ionic impurities with increasing tuning cycles, the stop-band position at certain voltages didn't remain constant and the tuning range became narrower.[11] The number of diffused ions and the ion diffusion length increase because the ionic species are continuously produced as the color tuning cycle is repeated. Therefore, efforts should be made to prevent or at least minimize the diffusion of the ions in order to develop robust tunable photonic crystals because the electrical double layer on the charged nanoparticles gets thinner with increasing ionic impurities in dispersion medium.[13]

To overcome this drawback, we developed an effective method of not only protecting ITO surfaces but also reducing the concentrations of H^+ and OH^- ions produced at the anode and cathode surfaces, respectively. We found that the voltage-driving methodology was an important factor to improve the tuning stability. As is shown in **Figure 2**(a) and (b), the stability depends on how the voltage was applied. 3.2 V of the voltage was applied as a square waveform in Figure 2(a) and as a triangle waveform in Figure 2(b), respectively. The photonic color responded very quickly (i.e., the photonic stop-band blue-shifted within 500 ms) during forward operation and recovered more slowly (i.e., it recovered to its original position in ~8 s) when the square-waveform voltage was applied for 2 s between 15 s intervals during which no voltage was applied, as shown in Figure 2(a). The same tuning experiments were repeated over 1000 times, and the peak positions were monitored and recorded every 12 ms. Electrostatic repulsion of the nanoparticles played a key role in the color reverting to the original when the electric field was removed. Strong electrostatic

© 2014 WILEY-VCH Verlag GmbH & Co. KGaA, Weinheim

repulsion became the only dominant force between the charged nanoparticles, and the inter-particle distance reverted to the original because of the force of restitution originating from the repulsion between adjacent nanoparticles. The degree of overlap between the electrical double layer on each nanoparticle surface is therefore very important in this event, and the significant decrement in the tuning range after 250 switching cycles (bottom plot of Figure 2(a) and (b)) is supposed to be due to the decreased surface charge and the electric double layer thickness caused by the increased concentration of ionic species in the dispersion. The response time was also slower with increasing number of tuning cycles (for example, 1.4 s after 100 switching cycles), which is supposed to be due to the same reason.

On the other hand, the voltage was continuously increased and decreased in Figure 2(b), forming a triangular waveform. Careful inspection of the initial switching profile shown in the middle plot reveals a threshold in the blue-shift phase with increasing voltage, while the stop-band shifts almost linearly with decreasing voltage. In addition, the switching stability was greatly improved and the stop-band position was almost same as the original one after 250 switching cycles, as is shown in the bottom figure. The improved stability when the triangular waveform was applied may be due to shorter exposure to voltage above the minimum equilibrium potential required for hydrogen-oxygen electrolysis (i.e., over-potential (E_0) = 1.23 V), a condition required for the production of ions. The stop-band tuning is accompanied by current flow because the movement of the colloidal nanoparticles corresponds to the movement of mobile charge in the dispersion.[12] Therefore, the change in the amount of current flow is closely related with the movement of the stop-band position, as is shown in Figure 2(c). The current flow exhibit maximum when the peak wavelength changes ($\Delta\lambda$) dramatically.

The electric double layer obtained using the modified Gouy-Chapman model was 240 nm thick. This means a significant amount of overlap existed between the electric double layers on the nanoparticle surfaces (green: 109 nm, red: 156 nm) because the inter-particle gaps in the green and red photonic crystals were 247 and 294 nm, respectively (see Figure S3). The Coulombic interaction between an isolated pair of similarly charged spheres is purely repulsive in this condition. Owing to the long range nature of the screened Coulombic interaction, the pair energy in monodisperse charged system can be expressed as[13]

$$V(r) = \frac{(Z * e)^2}{(4\pi \in_0 \in_r)} \left(\frac{\exp(ka)}{1+ka} \right)^2 \frac{\exp(-kr)}{r} \quad (1)$$

where V represents potential energy of the interaction, a represents the radius of the sphere, k represents the thickness of the electric double layer, r represents the inter-particle distance, and Z^* represents the effective charge of the nanoparticle. This equation indicates that the thinner electrical double layer is a major factor contributing to weakened interaction potential.

When the ionic concentration reaches critical level, the adjacent colloidal nanoparticles do not repel one another and the crystalline order can deteriorate. In addition, the electrophoretic movement of the nanoparticles decreases, significantly narrowing the tuning range. Furthermore, it is difficult for the stop-band position to revert to the initial one, and a gap exists between the positions of the stop-band during forward and backward operations. **Figure 3**(a,c) show that the stop-band position uncontrollably oscillates as a function of applied potential after a certain number of tuning cycles when bare ITOs were used as electrodes. Figure S4 more clearly shows detailed changes in the stop-band peak position when the stable tuning deteriorates. The narrowed tuning range and the gap in the stop-band position prevent the photonic crystal from being applied in practical devices.

To improve the switching characteristics of the photonic crystal, we coated a thin layer of ion-exchange resin membranes onto the surface of both electrodes in order to block the diffusion of the ions produced into the colloidal dispersion. To observe the effect of the ion-exchange resin coating on ITO on the switching reliability of the photonic crystal, we prepared green and red colloidal dispersions and tuned their colors to blue. The ionic-exchange membrane layer is supposed to block the diffusion of the ions produced at electrode surfaces. A Nafion® proton-exchange membrane (PEM) layer was coated onto the cathode surface to block the diffusion of OH^- ions, whereas a fumasep® (FAS) anion-exchange membrane (AEM) layer was coated onto the anode surface to block the diffusion of H^+ ions, as is illustrated in Figure 1(a). The thickness of each membrane layer was optimized through rigorous experiments; in which the thickness was varied from 30 to 400 nm. Various combinations of ion-exchange resins were also tested to maximize the efficiencies of the membranes toward blocking the diffusion of ions produced at the electrode surfaces. It is worth noting that the resistivity of the Nafion and FAS layers are lower than 10 Ω cm, which is promising in terms of the tuning range.

Figure 3 shows a summary of the selected stability data for the systems produced with either bare or ion-exchange resin-coated ITO for both electrodes. Switching from green to blue is clearly more stable than switching from red to blue because the degree of overlap of the electric double layer on the surface of the green colloid dispersions is higher than that of red ones because the inter-particle distance for the green colloid is shorter than that for the red one. In addition, switching from green to blue produced a lower concentration of ionic impurities in the dispersion than switching from red to blue did because switching from green to blue requires a lower voltage than switching from red to blue does. Using bare ITO for both electrodes resulted in only 60 fairly stable switching cycles (Figure 3(a)). On the other hand, using a cathode coated with a 200 nm-thick layer of PEM and an anode with a hybrid bilayer composed of an internal 30 nm-thick layer of AEM together with an external 200 nm-thick layer of PEM resulted in 320 stable switching cycles (Figure 3(b)). The green colloid showed the same tendency, but the number of stable switching cycles exhibited increased dramatically from 100 to 800 after modification of both ITOs with ion-exchange resins. In addition, the reliability of tuning the green colloid was greatly improved after the initial 100 tuning cycles. Figure 3(d) exhibits very stable and robust tuning behavior even after 800 times of switching cycles. Figure 3(e) shows a summary of the tuning stability data for the systems produced using: (1) two bare ITO electrodes, (2) a PEM-coated cathode and a bare ITO anode, and (3) a PEM-coated cathode and an AEM/PEM-coated anode. This data indicates

© 2014 WILEY-VCH Verlag GmbH & Co. KGaA, Weinheim

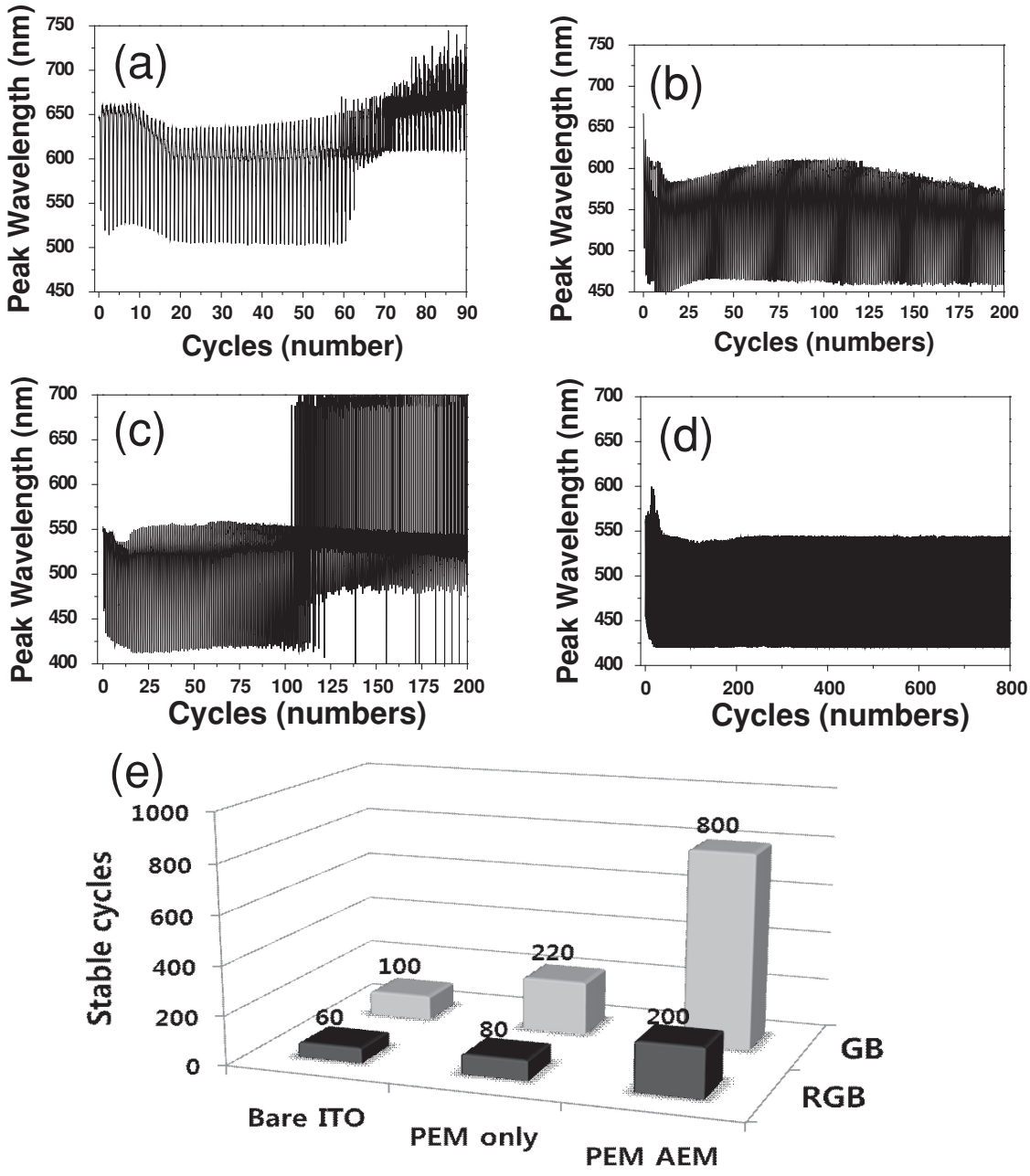

Figure 3. Stability test results for CCA devices fabricated with various colloid concentrations and under various electrode conditions. PS nanoparticle dispersions showing reflection peak at 650 nm were applied for voltage sweep (1 V/s) to express red, green, and blue: (a) Trace of the stop-band position change as a function of tuning cycle using uncoated ITOs on both electrodes (b) Trace of the stop-band position change as a function of tuning cycle using ion-exchange resin-coated ITOs on both electrodes. PS nanoparticle dispersions showing reflection peak at 550 nm were tested between bare ITO electrodes (c), and ion-exchange resin-coated ITOs on both electrodes (d). (e) Summary of the maximum number of switching cycles obtained by using ITO only electrodes, PEM layer coating on cathode and bare ITO on anode, and coated layers on both electrodes.

that the ion-exchange layer coatings significantly increased the number of stable tuning cycles. Using only the PEM-coated cathode as a cathode with the bare ITO anode also resulted in better tuning stability than using two bare ITO electrodes.

To investigate whether the coating layer on the electrode surfaces had blocked or suppressed the diffusion of ions into the colloidal dispersion, we used several test cells composed of various electrodes, each containing aqueous solutions of phenol red in order to directly monitor the pH in the cell during the tuning cycles by measuring the UV-absorbance spectrum for the test cell. The pH had previously been calibrated based on the ratios of the absorption peak maxima (absorption (550 nm)/ absorption (430 nm)) for phenol red under acidic and basic conditions, respectively (Figure S5). The change in pH was then recorded in situ when voltage was applied to the cell. The pH in the cell composed of two bare ITO electrodes almost remained

© 2014 WILEY-VCH Verlag GmbH & Co. KGaA, Weinheim

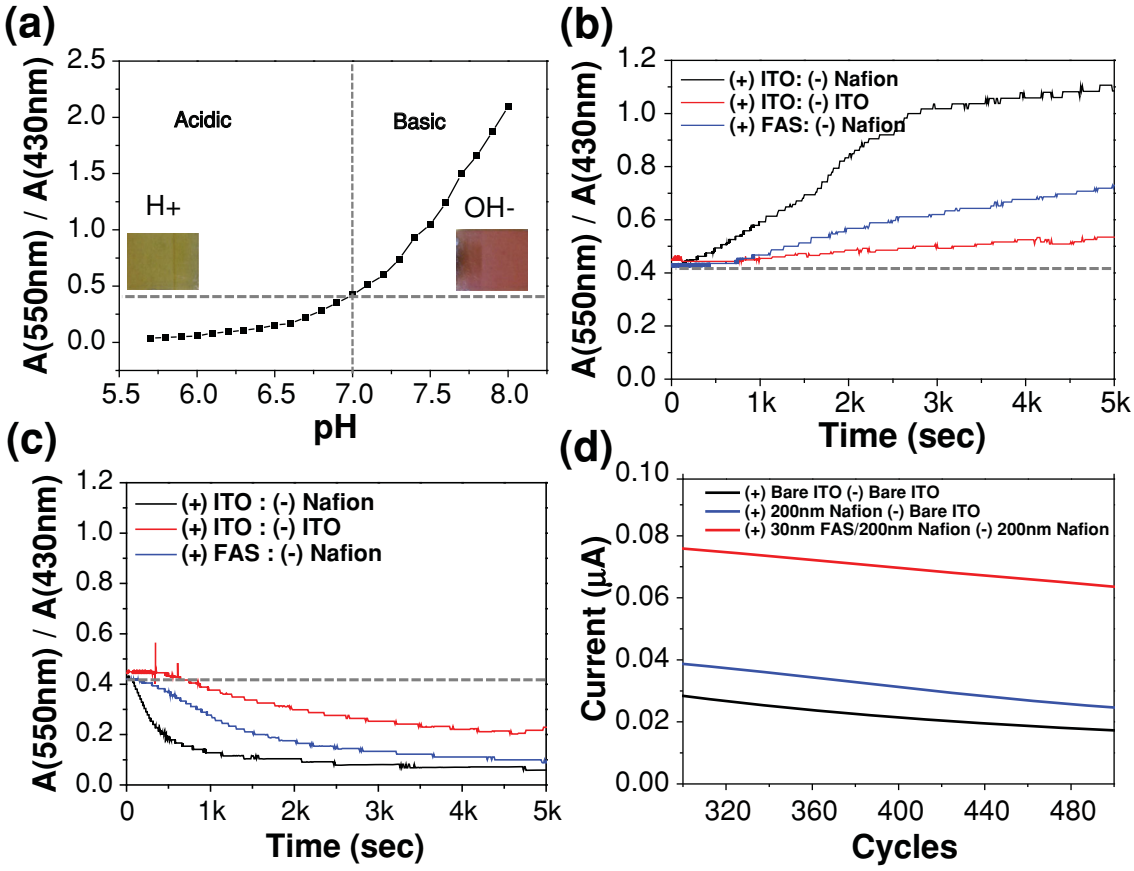

Figure 4. (a) Calibration curve for pH determined by ratios of absorbance peak maxima for acidic and basic phenol red. The dashed line indicates pH 7. The change in the absorbance ratio with increasing time during the application of a 3.2 V field to the test cell (b,c): (b) shows the data measured from the cathode side and (c) shows the data measured from the anode side. The measurement spot corresponding to the functions plotted in each figure are described in supporting Figure S6. (d) Current flow plotted as functions of number of operation cycles, as described in Figure 2(a).

constant; that is, the pH at the cathode monotonously increased until reaching ~7.1 (red line in **Figure 4**(b)) while the pH at the anode decreased until reaching 6.7 (red line in Figure 4(c)). The minor change in pH means almost symmetrical production of H^+ and OH^- ions at the anode and cathode surfaces, respectively.

The pH measured at the cathode side in a cell composed of bare ITO on anode and coated with a 200 nm-thick PEM layer on cathode increased to 7.3 after 5000 s (black line in Figure 4(b)), meaning that the OH^- ions produced were trapped in the PEM network. The pH measured for the anode side in the same cell, on the other hand, decreased because of the higher concentration of H^+ ions than OH^-. This result suggests that the PEM layer successfully worked as a good barrier against the diffusion of the ions produced at the electrode surfaces, especially the OH^- ions produced at the cathode surface. Cell composed of ion-exchange layer coating on both electrodes enabled the pHs at both coated electrodes to approach those at their bare-ITO counterpart (blue lines in Figure 4(b) and (c)), which means that the FAS layer in FAS/Nafion hybrid bilayer selectively blocked the diffusion of H^+ ions from anode, as is illustrated in Figure 1(a). Thick FAS-coated anode was unstable and significantly narrowed the tuning range owing to reduced magnitude of the internal electric field applied in colloidal dispersion. Hence, the hybrid composites coating composed of a 30 nm-thick internal layer of FAS on ITO and a 200 nm-thick external layer of PEM overcoating was used, showing the highest degree of ion blocking and the widest tuning range. This evidence further supports the hypothesis that OH^- ions were produced at the cathode surface and H^+ ions were produced at the anode surface and, therefore, that OH^- and H^+ ions were localized near the electrode surfaces. Figure 4(d) shows the changes in current flow during the tuning experiments. As is seen clearly in this figure, the amount of current flow is higher when the electrodes were effectively modified with ion-exchange resins to suppress diffusion of H^+ and OH^- ions. Therefore, the cell produced using both coated electrodes showed the highest current flow even after 1000 tuning cycles, meaning that the electrophoretic movement of the charged nanoparticles was effectively retained. It is worth noting that coating on cathode ITO with Nafion not only blocked the diffusion of OH^- ions but also protected the ITO from degradation such as opaque metallic indium formation and doping/dedoping of the ITO, which maintains ITO's electrical properties and enables stable switching over extended tuning cycles.

© 2014 WILEY-VCH Verlag GmbH & Co. KGaA, Weinheim

In conclusion, we have developed a robust and electrically tunable photonic crystal system composed of crystalline colloidal arrays through modification of the ITO electrode surfaces with ion-exchange resin layers, which acted as good barriers against ion diffusion and improved the tuning reliability. Using this technology combined with profound understanding of the tuning mechanism, we achieved more than 800 cycles of very reliable, wide-range (i.e., $\Delta\lambda > 100$ nm) photonic color switching for the first time. This technology may pave way to practical reflective display applications.

Experimental Section

The colloidal dispersion composed of 138 nm of polystyrene nanoparticles with a hydrophilic sulfate (-SO_4H) group on the surface was synthesized through modified emulsion polymerization similar to the procedure reported earlier.[10c] The synthesized colloidal dispersions were purified through dialysis at 60 °C for over a month to obtain ultra-pure particle dispersion by removing any unreacted monomers, surfactant, and other ionic impurities. The solid content of the particle was 12.6% and the particle concentration of the colloids was calculated to be 5.8×10^{13} cm^{-3}. The particle size distribution was measured by Transmission Electron Microscopy (TEM) and Dynamic Light Scattering (DLS). Zeta-potential of the colloid was determined using a ZetaPlus zeta-potential analyzer (Brookhaven Co.) from diluted colloids with de-ionized water. The colloidal dispersion exhibits brilliant reflective color after mixing with ion-exchange resin bead. By diluting this colloidal dispersion with de-ionized water, colloidal arrays with various colors could be easily prepared as is shown in Figure S3. After removing the ion-exchange resin bead, the colloidal dispersion was then injected between two sputter-patterned (15 Ω/□) parallel plates of ITO-coated glass separated by a 100-μm gap to form the test cell. In order to modify ITO electrodes, a Nafion117 solution (Sigma-Aldrich, 5% solution) was spin-cast at 4000 rpm,[14] forming PEM thin film on the surface of the patterned ITO electrode. AEM film with 30 nm thickness was prepared by spin-coating of 1 wt% FAS solution (FuMA-Tech GmbH) diluted with *N*-methyl-2-pyrrolidone (NMP). The reflection spectrum for the tunable photonic crystal cell was measured using an Ocean Optics USB 4000 connected to a cyclic voltammeter (CHI660D, CH Instruments, Inc.) in order to supply electrical potential. The optical response was monitored every 12 ms, and the stop-band peak position was simultaneously recorded using home-made software. Electro-deposition module in the COMSOL multiphysics software was used to simulate ion diffusion behavior and accumulated ion concentration under triangular pulses of electric voltage.

Supporting Information

Supporting Information is available from the Wiley Online Library or from the author.

Acknowledgements

M. G. Han and C.-J. Heo contributed equally to this work.

Received: January 26, 2014
Revised: February 25, 2014
Published online: March 25, 2014

[1] a) S. John, *Phys. Rev. Lett.* **1987**, *58*, 2486; b) E. Yablonovitch, *Phys. Rev. Lett.* **1987**, *58*, 2059.
[2] a) J. D. Joannopoulos, P. R. Villeneuve, S. Fan, *Nature* **1997**, *386*, 143; b) Y. Akahane, T. Asano, S. Noda, *Nature* **2003**, *425*, 944; c) P. Lodahi, A. F. Van Driel, I. S. Nikolaev, A. Irman, K. Overgaag, D. Vanmaekelbergh, W. L. Vos, *Nature* **2004**, *430*, 654; d) H. Zhang, X. Yu, P. B. Braun, *Nat. Nanotechnol.* **2011**, *6*, 277; e) J. J. Wiere Jr., A. David, M. M. Megens, *Nat. Photonic.* **2009**, *3*, 163; f) D.-H. Ko, J. R. Tumbleston, L. Zhang, S. Williams, J. M. DeSimone, R. Lopez, E. T. Samulski, *Nano Lett.* **2009**, *9*, 2742.
[3] a) A. C. Arsenault, D. P. Puzzo, I. Manners, G. A. Ozin, *Nat. Photonincs* **2007**, *1*, 468; b) J. Ge, Y. Hu, Y. Yin, *Angew. Chem. Int. Ed.* **2007**, *46*, 7428; c) Y. Kang, J. J. Walish, T. Gorrishnyy, E. L. Thomas, *Nat. Mater.* **2007**, *6*, 957.
[4] a) J. H. Holtz, S. A. Asher, *Nature* **1997**, *389*, 829; b) Y. Huang, F. Li, M. Qin, L. Jiang, Y. Song, *Angew. Chem. Int. Ed.* **2013**, *52*, 7296; c) N. Ganesh, W. Zhang, P. C. Mathias, E. Chow, J. A. N. T. Soares, V. Malyarchuk, A. D. Smith, B. T. Cunningham, *Nat. Nanotechnol.* **2007**, *2*, 515; d) C. Fenzl, T. Hirsch, O. S. Wolfbeis, *Angew. Chem. Int. Ed.* **2014**, DOI: 10.1002/anie.201307828.
[5] a) S. Furumi, T. Kanai, T. Sawada, *Adv. Mater.* **2011**, *23*, 3815; b) J. R. Lawrence, Y. Ying, P. Jiang, S. H. Foulger, *Adv. Mater.* **2006**, *18*, 300.
[6] a) C. I. Aguirre, E. Reguera, A. Stein, *Adv. Funct. Mater.* **2010**, *20*, 2565; b) J. Ge, Y. Yin, *Angew. Chem. Int. Ed.* **2011**, *50*, 1492; c) E. P. Chan, J. J. Walish, A. M. Urbas, E. L. Thomas, *Adv. Mater.* **2013**, *25*, 3934.
[7] K. Hwang, D. Kwak, C. Kang, D. Kim, Y. Ahn, Y. Kang, *Angew. Chem. Int. Ed.* **2011**, *50*, 6311.
[8] J. Huang, C. Tao, Q. An, W. Zhang, Y. Wu, X. Li, D. Shen, G. Li, *Chem. Commun.* **2010**, *46*, 967.
[9] a) S. A. Asher, J. Holtz, L. Liu, Z. Wu, *J. Am. Chem. Soc.* **1994**, *116*, 4997; b) K. Ueno, A. Inaba, Y. Sano, M. Kondoh, M. Watanabe, *Chem. Commun.* **2009**, *45*, 3603; c) M. G. Han, S. H. Foulger, *Adv. Mater.* **2004**, *16*, 231.
[10] a) T. S. Shim, S.-H. Kim, J. Y. Sim, J.-M. Lim, S.-M. Yang, *Adv. Mater.* **2010**, *22*, 4494; b) M. G. Han, C. G. Shin, S.-J. Jeon, H. Shim, C.-J. Heo, H. Jin, J. W. Kim, S. Lee, *Adv. Mater.* **2012**, *24*, 6438; c) M. G. Han, C.-J. Heo, C. G. Shin, H. Shim, J. W. Kim, Y. W. Jin, S. Lee, *J. Mater. Chem. C.* **2013**, *1*, 5791.
[11] H. Shim, C. G. Shin, C.-J. Heo, S.-J. Jeon, H. Jin, J. W. Kim, Y. W. Jin, S. Lee, J. Lim, M. G. Han, J.-K. Lee, *Appl. Phys. Lett.* **2014**, *104*, 051104.
[12] H. Shim, J. Lim, C. G. Shin, S.-J. Jeon, M. G. Han, J.-K. Lee, *Appl. Phys. Lett.* **2012**, *100*, 063113.
[13] R. Goldberg, H. J. Schöpe, *Chem. Mater.* **2007**, *19*, 6095.
[14] S. E. Andria, J. N. Richardson, N. Kaval, I. Zudans, C. J. Seliskar, W. R. Heineman, *Anal. Chem.* **2004**, *76*, 3139.

© 2014 WILEY-VCH Verlag GmbH & Co. KGaA, Weinheim